Journal of Materials Science: Materials in Electronics (2019) 30:2847–2853
https://doi.org/10.1007/s10854-018-0561-4

Sintering characteristics and microwave dielectric properties of $(Zr_{0.8}Sn_{0.2})TiO_4$ ceramics doped with La_2O_3 and MgO

Bo Chen[1] · Ling Han[2] · Baoyin Li[1]

Received: 4 October 2018 / Accepted: 12 December 2018 / Published online: 19 December 2018

Abstract
To investigate how addition of La_2O_3 and MgO influenced the structures, phase composition, sintering characteristics, and microwave dielectric properties of $(Zr_{0.8}Sn_{0.2})TiO_4$ (ZST) ceramics, we synthesized the ceramic samples using solid-state methodology. X-ray diffraction analysis indicated that the doped ZST samples were homogeneous, composed of a single phase with orthorhombic structure. Appropriate content of MgO doping favored grain growth and densification, affected the grain size distribution, and improved the dielectric properties of sintered ZST ceramics. With the sequentially increased in La_2O_3 and MgO contents, a defective ceramic including incomplete growth of grains, the incompact structures and the increasing porosities was formed. To demonstrate excellent microwave dielectric properties, 0.5 wt% La_2O_3 and 1.0 wt% MgO were added to ZST ceramics and sintered at 1320 °C for 5 h. Resulting sintered material had a moderate relative permitivitty ($\varepsilon_r = 38.44$), a superior $Q \times f$ value (52670 GHz at 5.6 GHz), and almost zero value for temperature coefficient of resonance frequency ($\tau_f = 0.81$ ppm/°C).

1 Introduction

With the ongoing revolution of 4G/5G microwave-based communication, direct broadcasting satellite and microelectronic technologies, the requirement of multifunctional integration and high power miniaturization of microwave devices have broadly increased [1–3]. Especially, microwave dielectric ceramics have gained extensive attraction over the past decade due to the rapid development of wireless communication technology. The demand of technology progress provides a tremendous opportunity with $(Zr_{0.8}Sn_{0.2})TiO_4$ (ZST) ceramics. To be specific, for qualify as a commercially viable candidate as microwave devices, ceramics should have a suitable relative permittivity (ε_r typically > 25) to largen signal velocity; a higher Q value to improve the transmission quality (Q typically > 3000) for decreasing the signal propagation delay time and suppress signal damping; a near-zero temperature coefficient ($\tau_f \sim 0$ ppm/°C) for temperature stability of the frequency response across temperature changes [4]. However, the raw materials, the dopants, and the microstructures play a significant role in above-mentioned properties of ZST ceramics [5–8]. It is almost impossible to prepare complete densified ZST ceramics without any sintering aid. Plenty of scientists have put energy into the role of dopants (e. g., $Ba_3(VO_4)_2$, MgO and SrO) and their influence on microwave dielectric loss in ZST ceramics [9–11]. Recently, Zhang et al. [9] investigated that adding 0.5 wt% $Ba_3(VO_4)_2$ addition in ZST ceramics showed good microwave dielectric properties of $\varepsilon_r = 36.6$, $Q \times f = 46{,}000$ GHz, $\tau_f = 1.47$ ppm/°C with 1275 °C sintering temperature. The microwave dielectric properties of ZST ceramics doped with 0.2 wt% MgO, 0.6 wt% SrO and 1.0 wt% La_2O_3 at 1300 °C ($\varepsilon_r \sim 40.11$, $Q \times f \sim 51{,}000$ GHz and $\tau_f \sim -2.85$ ppm/°C) have been reported by Sun et al. [10]. Qian et al. [11] synthesized ZST ceramics by adding 1.0 wt% La_2O_3, 0.6 wt% MgO and 0.4 wt% BaO to form material with comprehensive performance of ε_r of 38.68, a $Q \times f$ value of 42,300 GHz and a τ_f value of +5.4 ppm/°C when sintered at 1340 °C.

Kim et al. [12, 13] published that a large number of the alkaline earth metal oxides (e.g., CaO, MgO, SrO or BaO) and TiO_2 formed eutectic liquids and $[TiO_4]$ tetrahedron at sintering temperature below 1400 °C, as a result, these oxides availably reduced fabricating cost of ZST ceramics. Previous studies showed that the addition of La^{3+} ions

✉ Bo Chen
chenbo0538@126.com

[1] College of Mechanical Engineering, Shandong University of Science and Technology, Taian Campus, Taian 271000, China

[2] Taian City Central Hospital, Taian 271000, China

influenced the dielectric properties of ZST materials [14]. Ioachim et al. [15] elaborated that the MgO doped ZST samples showed an extremely tiny decrease of the dielectric constant from 1 kHz to 6.5 GHz of less than 1%. However, there was also an exceptional thermal stability of the dielectric constant, in the temperature range − 150–150 °C of 6–7 ppm/°C. Nevertheless, La^{3+} (added as La_2O_3) in combination with divalent Mg ion (MgO) isn't tested as binary dopants in ZST ceramics. This work aimed to thoroughly examine how addition of lanthane (III)-oxide and magnesium oxide influenced structures, phase composition, sintering characteristics, and microwave dielectric properties of ZST materials. The goal was to find the optimal contents of dopants that yielded sintered material with the excellent temperature coefficient of the frequency of resonance.

2 Experimental procedure

ZST ceramics were synthesized by conventional solid state reaction route. The starting powders used in this study were ZrO_2 (99.9%, Jinkun Co., Ltd., Zhejiang, China), SnO (99.9%, Haozhao Chemical Co., Ltd. Guangdong, China), TiO_2 (99.9%, Yuxing Chemical Co. Ltd., Shandong, China), La_2O_3 (99.9%, Ganzhou Kemingrui Non-ferrous Materials Co., Ltd. Jiangxi, China) and MgO (99.9%, Weifang Xuhui New Materials Co. Ltd., Shandong, China). The weight percent of La_2O_3 and MgO were tabulated in Table 1. The ratio of La_2O_3 and MgO was kept as 1 to 2 in all samples. The various kinds of raw materials were weighed according to their stoichiometric and mixed with deionized water in Si_3N_4 bottles. After that, the mixed slurries were slowly dried in water bath kettle at 60 °C and then calcined at different temperature (950 °C, 1050 °C and 1150 °C) for 3 h in air atmosphere. After breaking and remilling monolithic calcined block, they were sieved through 60 mesh, the fine powders together with the 5 wt% polyvinyl alcohol were uniaxially compacted into a cylinder mould of 13.1 mm in diameter and 7.0 mm in thickness at 150 MPa pressure. To remove the polyvinyl alcohol, we adjusted the heating program at 450 °C for 5 h and then sintered in the temperature range of 1280–1360 °C for 5 h in air after putting the green bodies into high temperature sintering furnace. The rate of rise of temperature was 1 °C/min.

Table 1 Mass fraction and number of La_2O_3 and MgO in each sample

Sample	La_2O_3 /wt%	MgO /wt%
LM_1	0.25	0.5
LM_2	0.5	1.0
LM_3	0.75	1.5
LM_4	1.0	2.0

The relative density and crystal structure of sintered ceramics were determined by the Archimedes method and X-ray diffraction equipment (XRD; RIGAKU; Smartlab 3) with CuKα radiation from 10°–80° range in 2θ, respectively. The microstructures of the sintered material were visualized by scanning electron microscope (Quanta 200 FEG, FEI Co., USA). A network analyzer (N5234A, Agilent Co., Ltd., USA) was evaluated the microwave dielectric properties of the samples. The relative permittivities were measured using the Hakki–Colemanpost–resonator method [16] by exciting the TE_{011} resonant mode of the DR using the electric probe of an antenna as suggested by Courtney [17]. The TE_{011} mode of the cavity method was used to determine the unloaded quality factors [18]. All measurements were made in the frequency range of 2–8 GHz at room temperature. The τ_f values of the TE_{011} mode were acquired from 25 °C to 80 °C. The τ_f values were calculated as:

$$\tau_f = \frac{1}{f_{25}} \times \frac{f_{80} - f_{25}}{80 - 25} \quad (1)$$

where f_{80} and f_{25} figure as the resonant frequencies at corresponding temperatures.

3 Results and discussion

3.1 X-ray diffraction analysis

Figure 1 illustrated the XRD patterns of pure ZrO_2, SnO_2 and TiO_2 mixed powders sintered at various calcination

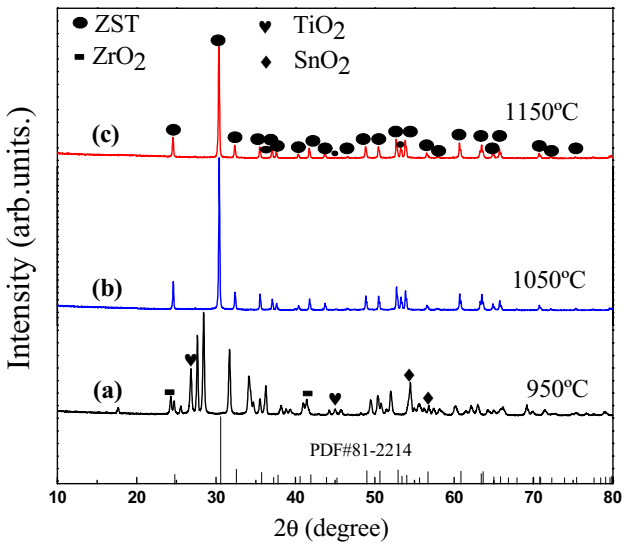

Fig. 1 XRD patterns of pure ZrO_2, SnO_2 and TiO_2 mixed powders calcined at a 950 °C, b 1050 °C and c 1150 °C for 3 h in air, respectively

temperature for 3 h. Pattern (a) showed the XRD profile of the compacted powders calcined at 950 °C, a orthorhombic structured ZST phase was predominantly identified (JCPDS Card No. 81-2214) by the circles, however, peaks corresponding to small contents of unreacted ZrO_2, SnO_2 and TiO_2 phases were also observed in the profile of the pattern (a). From the pattern (b) and (c), when the compacted powers calcined at 1050 °C or 1150 °C, it could be found that the intensity of ZST phase diffraction peaks moved to a larger angle and decreased apparently without formation of unreacted raw materials phase, indicating that orthorhombic structure increased continuously and pure ZST ceramics would be obtained. All the diffraction peaks in pattern (c) resembled in pattern (b). Wang et al. [19, 20] reported that the relative higher calcined temperature was benefit for the reaction of the main ZST phase. Thus, in order to obtain pure orthorhombic structure, the calcination temperature of ZrO_2, SnO_2 and TiO_2 mixed powders were employed to 1150 °C for 3 h in air in the subsequent experiments.

Figure 2 presented the powder XRD patterns of ZST ceramics sintered at 1320 °C prepared with different levels of La_2O_3 and MgO. From the left-hand side figure, it was evident that all the samples prepared at 1320 °C had extremely similar XRD patterns, with a splitting of diffraction peaks at $2\theta \approx 32.7°$. We could not find any impurity peaks in XRD patterns, proving that the sintered ZST ceramics not contained redundant impurity phase. Observed splitting of diffraction peaks corresponded to (111) planes of homogeneous ZST phase, with the space group *Pbcn* standard JCPDS, file No. 81-2214 of orthorhombic structure. The doping mechanism of ZST ceramics was also investigated. As can be seen from the magnified (111) peaks on right-hand side, the (111) Bragg peaks showed slightly reduced 2θ angles with the increasing La_2O_3 and MgO contents. To calculate the lattice parameters of the unit cell, we used Rietveld method to refine the diffractograms of ZST ceramics. All parameters

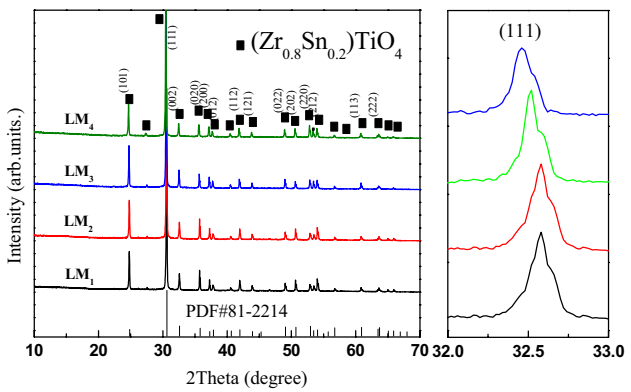

Fig. 2 Powders XRD patterns of ZST ceramics sintered at 1320 °C with different contents of La_2O_3 and MgO

Table 2 Lattice parameters and unit cell volumes of ZST samples

Sample	Sintering temperature /°C	a_0 /nm	b_0 /nm	c_0 /nm	Unit cell volume V_0/ nm^3
LM_1	1320	0.4863	0.4765	0.5510	0.12768
LM_2	1320	0.4984	0.4698	0.5463	0.12792
LM_3	1320	0.4717	0.4789	0.6310	0.14254
LM_4	1320	0.4992	0.5012	0.5777	0.14454

listed in Table 2 were calculated accordingly. The continuous increase in lattice parameters was observed. The unit cell volume of LM_4 was 0.14454 nm^3, while unit cell volumes of LM_1, LM_2 and LM_3 were 0.12768 nm^3, 0.12792 nm^3 and 0.14254 nm^3, respectively. According to the ionic radius tolerance principle, this phenomenon can be explained by the larger volume of La^{3+} ion (0.1172 nm) compared to Zr^{4+} (0.072 nm), Sn^{4+} (0.069 nm) and Ti^{4+} (0.0605 nm). The increased contents of La_2O_3 and MgO led to the larger unit cell volumes, which was consistent with the lower shift of diffraction peaks according to the Bragg's equation.

3.2 Scanning electron micrograph

Typical SEM micrographs of the fractured surfaces of ZST ceramics with different contents of La_2O_3 and MgO sintered at 1320 °C for 5 h were depicted in Fig. 3a–d. The white points in Fig. 3d were caused by the metal spraying process. Well densified and homogenous ceramics were observed in LM_1 and LM_2 samples, suggesting the high densification when sintered at optimum temperature. With the increased of La_2O_3 and MgO contents, the small grains gradually grew up and the size distribution of crystalline grains became more uniform (Fig. 4b). In addition, Fig. 4b showed a low-porous, dense material, suggesting that the minuscule contents of dopants (La_2O_3 and MgO) favored the densification of ZST ceramics. Further addition of La_2O_3 and MgO produced an excessive grain growth. As indicated in Fig. 3c and d, LM_3 and LM_4 samples sintered at 1320 °C showed visible pores and incomplete microstructure, resulting in an insufficient densification. Furthermore, as can be notably seen in Fig. 3b and c, LM_2 sample compared with LM_3 sample, clearly exhibited legible grain boundaries, however, some of the LM_3 sample grains were distorted, and such grains in Fig. 3a and b were not found. Excessive content of MgO might lead to local heterogeneity in composition and liquid phase formation at certain, microscopic parts of ceramics [21]. Besides, the abnormal grain growth might impair the dielectric characteristics of ZST ceramics.

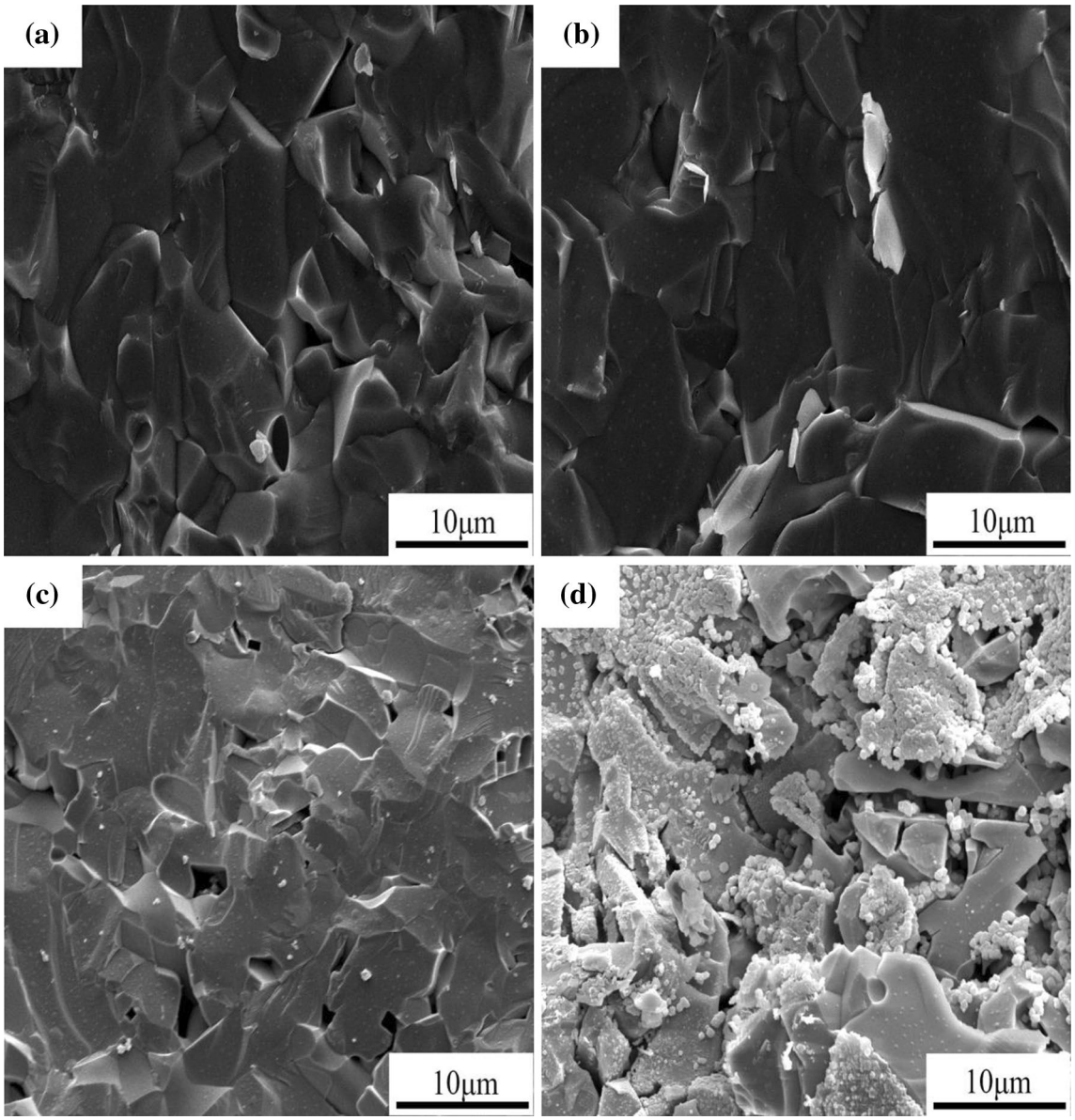

Fig. 3 SEM micrographs on fractured surfaces of ZST ceramics with **a** LM_1, **b** LM_2, **c** LM_3, **d** LM_4 sintered at 1320 °C for 5 h

3.3 Sintering characteristics

Figure 4 showed the temperature change in bulk densities (ρ) of ZST materials doped with different contents of La_2O_3 and MgO. The sintering of ZST ceramics was a densification process [22]. For all ceramic samples, the increase in temperature led to densification of a material, with the maximum density reached at 1320 °C. For higher temperatures, the bulk densities decreased due to over-sintering. When 0.25 wt% La_2O_3 and 0.5 wt% MgO were added, the bulk densities were relatively low, and the densities increased with the La_2O_3 and MgO contents increasing.

The maximum bulk density of LM_2 sample was 5.08 g/cm^3, reaching 97.88% of the theoretical value for pure ZST (5.19 g/cm^3). Additionally, for LM_3 and LM_4 samples, increased contents of La_2O_3 and MgO decreased the bulk densities, probably owing to the production of liquid phase and subsequent formation of more porous grains (Fig. 3c–d). The degradation of the bulk densities was mainly due to formation of liquid phase as a consequence of the increased content of MgO. This was in accordance with previous studies of Pamu et al. [23].

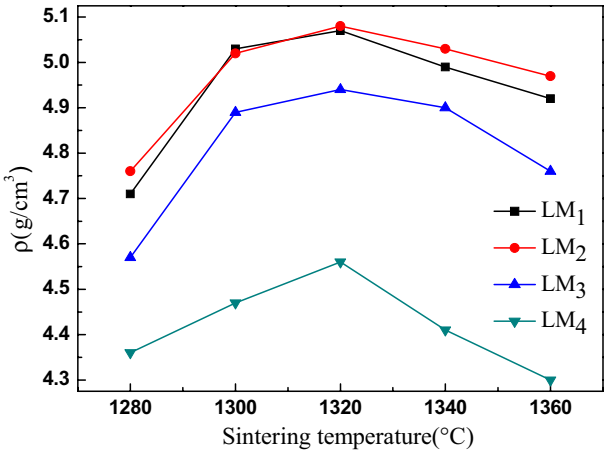

Fig. 4 Bulk densities (ρ) of ZST ceramics with various contents of La_2O_3 and MgO as a function of sintering temperature

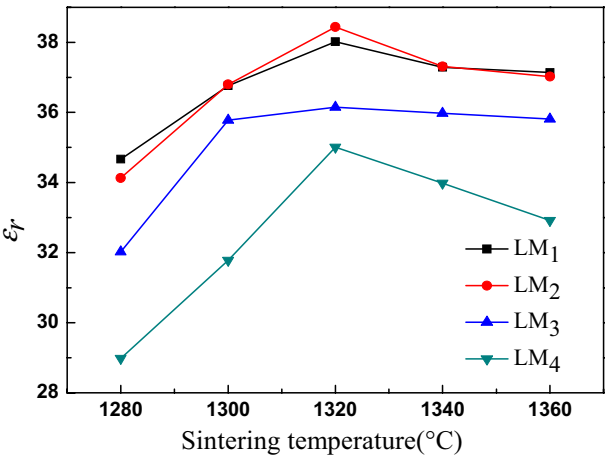

Fig. 5 The relative permittivity (ε_r) of ZST ceramics with various contents of La_2O_3 and MgO as a function of sintering temperature

3.4 Microwave dielectric properties

Figure 5 showed the temperature variation of relative permittivities (ε_r) of ZST materials, doped with increasing percentages of La_2O_3 and MgO. With the sintering temperature ranged from 1280–1360 °C, the ε_r values initially increased, reached a maximum at 1320 °C followed by the decreased at higher temperatures. The ε_r values varied from 28.98 to 38.44; and a maximum of 38.44 for LM_2 sample achieved at 1320 °C. The variation in relative permittivity followed the temperature trend of bulk density (Fig. 4).

Many intrinsic and extrinsic factors might influence ε_r values [5, 24–27]. In this report, the ε_r values of ZST ceramics obtained at different sintering temperatures varied only with bulk densities, as the materials were homogeneous, without the structural defects and formation of secondary structures. Additionally, increased MgO content led to decrease in the relative permittivities of ZST ceramics. The likely reason for this effect was the excess liquid phase formation in the ceramics. Regarding the intrinsic factors, the theoretical value for relative permittivity can be estimated from Clausius–Mossotti equation [28]:

$$\varepsilon_r = \frac{3V_M + 8\pi x}{3V_M - 4\pi x} \quad (2)$$

where V_M was unit cell volume and x was cell polarizability of ceramics. Unit cell polarizability was related to the expansion characteristics of ZST materials. The more voluminous ions with larger values for dielectric polarizability increased the cell polarizability of a material. Compared to normal constituents of ZST ceramics, La^{3+} was larger and also more polarizable (dielectric polarizability of La^{3+} was 6.07 Å^3 *vs*. 3.25, 2.83 and 2.93 Å^3 for Zr^{4+}, Sn^{4+} and Ti^{4+}, respectively) [29], which resulted in the increasing of the relative permittivity. The complete list of properties of ZST ceramics (Table 3) confirmed this observation.

Figure 6 demonstrated the temperature changes in $Q \times f$ product of ZST materials, doped with various percentages of La_2O_3 and MgO. The $Q \times f$ product varied with the reaction temperature similarly to the apparent bulk density (Fig. 4). More specifically, the $Q \times f$ values for all materials firstly rose up to the maximum values at 1320 °C, followed

Table 3 The list of bulk densities, relative permittivities, Q and τ_f values of ZST ceramics at different sintering temperatures and dopants percentages

Composition	Sintering temperature (°C)	ρ (g/cm^3)	ε_r	Q	τ_f(ppm/°C)	Ref
Pure ZST	1600	4.92	36.10	7000	0	[30]
0.25 wt%La_2O_3 + 0.5 wt%MgO	1280	5.07	38.02	8195	− 1.23	–
0.5 wt%La_2O_3 + 1.0 wt%MgO	1280	5.08	38.44	9410	0.81	–
0.75 wt%La_2O_3 + 1.5 wt%MgO	1280	4.94	36.15	6212	− 2.34	–
1.0 wt%La_2O_3 + 2.0 wt%MgO	1280	4.56	35.01	5585	2.06	–
0.25 wt%La_2O_3 + 0.5 wt%SrO	1310	5.10	39.56	7321	− 2.65	[2]
1.0 wt%La_2O_3 + 0.5 wt%CaO	1335	5.06	39.56	7875	− 1.66	[15]
1.0 wt%La_2O_3 + 2.0 wt%BaO	1350	5.10	41.00	9800	− 3.79	[30]

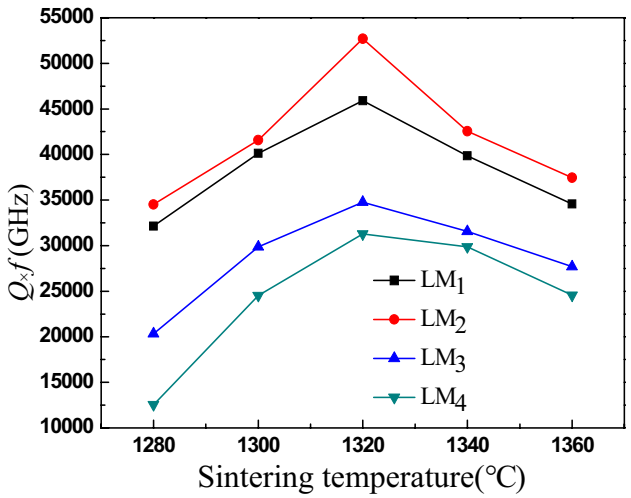

Fig. 6 The $Q \times f$ values of ZST ceramics with various contents of La_2O_3 and MgO as a function of sintering temperature

by the decreased at higher temperatures. At 1320 °C, LM_2 sample reached a maximum product of 52,670 GHz (at 5.6 GHz). At the same temperature, $Q \times f$ values of samples LM_3 and LM_4 were significantly lower (34,780 GHz and 31,280 GHz at 5.6 GHz, respectively).

The quality of ceramics was determined by the intrinsic and extrinsic losses in dielectric properties. Internal vibrations of the constituents of a material (atoms, ions, electrons) caused intrinsic loss, while the porosity, grain size, crystal defects, phase composition and phase transition yielded extrinsic losses in ceramics [31, 32]. As $Q \times f$ values varied with the temperature similarly to the bulk densities, it can be concluded that the densification decreased dielectric loss of sintered ZST materials.

The content of MgO added also influenced the dielectric properties of this material. The surplus MgO (1.5 wt% and 2.0 wt%) induced inhomogeneity in the microstructure of a material and decreased its overall quality. The findings of Pamu et al. confirmed the crucial role of MgO content optimization for obtaining the optimal dielectric properties of ZST ceramics [23].

The excessive addition of La_2O_3 also diminished the dielectric properties of ZST ceramics. The trivalent La^{3+} behaved as an acceptor and may create the oxygen vacancies within the structure of a material according to the following expression:

$$La_2O_3 \rightarrow 2La'_{Ti} + 3O_O + V^{\cdot\cdot}_O \quad (3)$$

The entrance of excess oxygen into the crystal structure of ZST ceramics impaired the homogeneity, leading to non-harmonic oscillations and decreased dielectric properties [33].

A comparison between the properties of undoped and doped ZST ceramics along with their sintering conditions, apparent densities, and microwave dielectric properties was provided in Table 3. The additives in the table varied in kind of the II A alkaline earth metal oxide (MgO, SrO, CaO and BaO). We found that adding a certain amount of MgO in our study not only conduced to reduce the sintering temperature of the ZST ceramics, but also demonstrated an insignificant decrease of Q value. Additionally, the temperature coefficients of the resonant frequency were − 1.23, 0.81, − 2.34, and 2.06 ppm/°C for LM_1, LM_2, LM_3, and LM_4 sintered at 1320 °C, respectively. The τ_f values had correlation to the ingredient and the impurity phases of the material [34]. ZST ceramics were temperature stable and dopants did not cause any impurity phases, the τ_f values did little alter with La_2O_3 and MgO contents added. According to the data listed in Table 3, LM_2 sample seemed to be the most suitable for application in microwave components, due to the relatively lower sintering temperature (1320 °C), small temperature coefficient of the resonant frequency (τ_f equal to 0.81 ppm/°C), moderate relative permittivity ($\varepsilon_r = 38.44$), and excellent dielectric properties ($Q \times f$ value equal to 52,670 GHz at 5.6 GHz).

4 Conclusions

The structures and microwave dielectric properties of ZST ceramics with various contents of La_2O_3 and MgO were investigated. The XRD patterns indicated a homogeneous material composed of single phase with orthorhombic structure. The size of unit cell increased with the increased La_2O_3 and MgO contents, for all materials examined. The optimal contents of La_2O_3 and MgO dopants were 0.5 wt% and 1.0 wt%, respectively. This combination led to the sintered material with the relatively lower sintering temperature (1320 °C), improved density and microwave dielectric properties. The correlation between the MgO content and the morphology, density and dielectric properties of ZST ceramics was also confirmed in this study. The near zero τ_f values of ZST ceramics can be obtained and had no significant change under different contents of dopants. After being sintered at 1320 °C for 5 h, the excellent microwave properties: $Q \times f$ value of ~ 52,670 GHz (at 5.6 GHz), the ε_r value of ~ 38.44, and the τ_f value of ~ 0.81 ppm/°C, were obtained for ZST ceramics with 0.5 wt% La_2O_3 and 1.0 wt% MgO. The doped ZST material optimized in this study might be applied as a constituent of microwave components.

Acknowledgements This work was supported by National Natural Science Foundation of China (No.51578327).

References

1. M. Xiao, Y.S. Wei, Q.Q. Gu, P. Zhang, The relationship between the bond ionicity, lattice energy, bond energy and microwave dielectric properties of $LaNbO_4$ ceramics. J. Mater. Sci. Mater. Electron. **29**(12), 9963–9970 (2018)
2. Q.L. Sun, H.Q. Zhou, X.F. Luo, L.S. Hu, L.C. Ren, Influence of La_2O_3/SrO doping of $(Zr_{0.8}Sn_{0.2})TiO_4$ ceramics on their sintering behavior and microwave dielectric properties. Ceram. Int. **42**(10), 12306–12311 (2016)
3. D.D. Liu, P. Liu, B.C. Guo, Low-temperature sintering and microwave dielectric properties of $Li_4Mg_3Ti_2O_9$ ceramics by a sol–gel method. J. Mater. Sci. **29**(12), 10264–10268 (2018)
4. S. Takahashi, A. Kan, H. Ogawa, Microwave dielectric properties and crystal structures of spinel-structured $MgAl_2O_4$ ceramics synthesized by a molten-salt method. J. Eur. Ceram.Soc. **37**(3), 1001–1006 (2017)
5. R.Y. Yang, M.H. Weng, H. Kuan, TEM observation of liquid phase sintering in V_2O_5 modified $Zr_{0.8}Sn_{0.2}TiO_4$ microwave ceramics. Ceram. Int. **35**(1), 39–43 (2009)
6. N. Michiura, T. Tatekawa, Y. Higuchi, H. Tamara, Role of donor and acceptor ions in the dielectric loss tangent of $(Zr_{0.8}Sn_{0.2})TiO_4$ dielectric resonator material. J. Am. Ceram. Soc. **78**(3), 793–796 (1995)
7. Y.C. Heiao, L. Wu, C.C. Wei, Microwave dielectric properties of (Zr,Sn)TiO_4 ceramic. Mater. Res. Bull. **23**(12), 1687–1692 (1988)
8. K. Wakino, K. Mino, H. Tamura, Microwave characteristics of (Zr,Sn)TiO_4 and BaO-PbO-Nd_2O_3-TiO_2 dielectric resonators. J. Am. Ceram. Soc. **67**(4), 278–281 (1984)
9. Z.Y. Zhang, H.K. Zhu, Y. Zhang, Y.H. Chen, Z.X. Fu, K. Huang, Q.T. Zhang, Effects of the $Ba_3(VO_4)_2$ additions on microwave dielectric properties of $(Zr_{0.8}Sn_{0.2})TiO_4$ ceramics. J. Mater. Sci. **28**(2), 2044–2048 (2017)
10. Q.L. Sun, H.Q. Zhou, L. Qian, Y.Z. Wang, H.K. Zhu, Z.X. Yue, Effects of MgO, SrO and La_2O_3 co-doping on structure and properties of $(Zr_{0.8}Sn_{0.2})TiO_4$ ceramics. J. Inorg. Mater. **31**(8), 812–818 (2016)
11. L. Qian, H.Q. Zhou, Q.X. Jiang, L.C. Ren, W.T. Xie, X.F. Luo, Q.L. Sun, Effect of MgO, BaO and La_2O_3 additions on microwave dielectric properties of $(Zr_{0.8}Sn_{0.2})TiO_4$ ceramics. J. Mater. Sci. **27**(6), 6183–6187 (2016)
12. D.J. Kim, J.W. Hahn, G.P. Han, S.S. Lee, T.G. Choy, Effects of alkaline-earth-metal addition on the sinterability and microwave characteristics of (Zr,Sn)TiO_4 dielectrics. J. Am. Ceram. Soc. **83**(4), 1010–1012 (2000)
13. Z. Wang, Q.F. Shu, K.C. Chou, Structure of CaO-B_2O_3-SiO_2-TiO_2 glasses: a Raman Spectral Study. ISIJ. Int. **51**(7), 1021–1027 (2011)
14. B. Chen, L. Han, B.Y. Li, X.D. Sun, Effects of CaO and La_2O_3 doping of $(Zr_{0.8}Sn_{0.2})TiO_4$ ceramics on the densifying behavior and microwave dielectric properties. J. Mater. Sci. **28**(13), 9542–9547 (2017)
15. A. Ioachim, M.G. Banciu, M.I. Toacsen, L. Nedelcu, D. Ghetu, H.V. Alexandru, C. Berbecaru, A. Dutu, G. Stoica, High-k Mg-doped ZST for microwave applications. Appl. Surf. Sci. **253**(1), 335–338 (2006)
16. B.W. Hakki, P.D. Coleman, A dielectric resonator method of measuring inductive capacities in the millimeter range. IEEE Trans. Microwave Theory Tech. **8**, 402–410 (1960)
17. W.E. Courtney, Analysis and evaluation of a method of measuring the complex permittivity of microwave insulators. IEEE Trans. Microwave Theory Tech. **18**, 476–485 (1970)
18. Y. Kobayashiy, M. Katoh, Microwave measurement of dielectric properties of low-loss materials by the dielectric rod resonator method. IEEE Trans. Microwave Theory Tech. **33**, 586–592 (1985)
19. G.Q. Wang, S.H. Wu, H.Y. Yan, Study on the calcination and sintering technique of $(Zr_{0.8}Sn_{0.2})TiO_4$ ceramics. Piezoelectrics Acoustooptics. **25**(4), 321–324 (2003)
20. L.Z. Wang, L.X. Wang, Z.F. Wang, B.Y. Huang, Q.T. Zhang, Z.X. Fu, Effect of ZnO/Er_2O_3 addition on microwave properties of $(Zr_{0.8}Sn_{0.2})TiO_4$ ceramics. J. Mater. Sci. **27**(4), 3929–3933 (2016)
21. J.Q. Chen, Y. Tang, H.C. Xiang, L. Fang, H. Porwald, C.C. Li, Microwave dielectric properties and infrared reflectivity spectra analysis of two novel low-firing $AgCa_2B_2V_3O_{12}$ (B = Mg, Zn) ceramics with garnet structure. J. Eur. Ceram. **38**(14), 4670–4676 (2018)
22. M. Mikoczyova, Influence of forming method and sintering process on densification and final microstructure of submicrometre alumina ceramics. Process. Appl. Ceram. **2**(1), 13–17 (2008)
23. D. Pamu, G.L.N. Rao, K.C.J. Raju, Effect of BaO, SrO and MgO addition on microwave dielectric properties of $(Zr_{0.8},Sn_{0.2})TiO_4$ ceramics. J. Alloy. Compd. **475**(1–2), 745–751 (2009)
24. C.L. Huang, S.H. Huang, Low-loss microwave dielectric ceramics in the $(Co_{1-x}Zn_x)TiO_3$ (x = 0-0.1) system. J. Alloy. Compd. **515**, 8–11 (2012)
25. Q.S. Cao, W.Z. Lu, X.C. Wang, J.H. Zhu, B. Ulla, W. Lei, Novel zinc manganese oxide-based microwave dielectric ceramics for LTCC applications. Ceram. Int. **41**(9), 9152–9156 (2015)
26. Z.Y. Zou, Z.H. Chen, X.K. Lan, W.Z. Lu, B. Ulla, X.H. Wang, W. Lei, Weak ferroelectricity and low permittivity microwave dielectric properties of $Ba_2Zn_{(1+x)}Si_2O_{(7+x)}$ ceramics. J. Eur. Ceram. Soc. **37**(9), 3065–3071 (2017)
27. X.S. Lyu, L.X. Li, H. Sun, S. Zhang, S. Li, High-Q microwave dielectrics in wolframite magnesium zirconium tantalate ceramics. Ceram. Int. **42**(1), 2036–2040 (2016)
28. R.D. Shannon, Dielectric polarizabilities of ions in oxides and fluorides. J. Appl. Phys. **73**(1), 348–366 (1993)
29. L. Fang, C.X. Su, H.F. Zhou, Z.H. Wei, H. Zhang, Novel low-firing microwave dielectric ceramic $LiCa_3MgV_3O_{12}$ with low dielectric loss. J. Am. Ceram. Soc. **96**(3), 688–690 (2013)
30. S.X. Zhang, J.B. Li, H.Z. Zhai, J.H. Dai, Low temperature sintering and dielectric properties of $(Zr_{0.8}Sn_{0.2})TiO_4$ microwave ceramics using La_2O_3/BaO additives. Mater. Chem. Phys. **77**(2), 470–475 (2002)
31. W.S. Kim, T.H. Kim, E.S. Kim, K.H. Yoon, Microwave dielectric properties and far infrared reflectivity spectra of the $(Zr_{0.8}Sn_{0.2})TiO_4$ ceramics with additives. Jpn. J. Appl. Phys. **37**(9B), 5367–5371 (1998)
32. Q.L. Sun, H.Q. Zhou, H.K. Zhu, H.Q. Qi, L.S. Hu, Z.X. Yue, Sintering behavior and microwave dielectric properties of Y_2O_3-ZnO doped $(Zr_{0.8}Sn_{0.2})TiO_4$ ceramics. J. Mater. Sci. **27**(8), 7750–7754 (2016)
33. R.K. Bhuyan, T.S. Kumar, D. Goswami, A.R. James, D. Pamu, Liquid phase effect of La_2O_3 and V_2O_5 on microwave dielectric properties of Mg_2TiO_4 ceramics. J. Electroceram. **31**(1–2), 48–54 (2013)
34. L.Z. Wang, L.X. Wang, Z.F. Wang, B.Y. Huang, Q.T. Zhang, Z.X. Fu, Effect of sintering aid ZnO-CeO_2 on dielectric properties of $(Zr_{0.8}Sn_{0.2})TiO_4$ ceramics. J. Mater. Sci. **26**(11), 9026–9030 (2015)